Stanisław Adamiak*, Wojciech Bochnowski, Andrzej Dziedzic, Ryszard Filip and Eugeniusz Szeregij

# Structure and Properties of the Aluminide Coatings on the Inconel 625 Superalloy

**Abstract:** The research samples used in this study were based on the Inconel 625 alloy; the examined samples were coated with aluminide films deposited in a low-activity chemical vapor deposition (CVD) process. The samples' microstructure was investigated with optical and electron microscopy and energy dispersive X-ray spectroscopy analysis. Hardness measurements were performed using Vickers and Berkovich test methods. The adhesion of the aluminide coating was determined by fractography. It was shown that the fracture mechanism was different for the respective zones of the aluminide coating and the substrate material. The outer zone of the aluminide coating is characterized by an intercrystalline fracture, with a small contribution of transcrystalline fracture within individual grains (large crystallites in the bottom of the zone, composed of smaller crystallites, also show an intercrystalline fracture). The substrate material exhibited a ductile intercrystalline fracture. Based on this investigation, an increase of the microhardness of the material occurring at loads below 0.2 N was observed. When determining microhardness of aluminide coating it is necessary to take into account the optimal choice of the indentation tip.

**Keywords:** CVD process, aluminide coating, Inconel 625, fracture material, micro- and nanohardness

**PACS.** 81. Materials science

DOI 10.1515/htmp-2014-0139
Received August 11, 2014; accepted January 5, 2015

***Corresponding author: Stanisław Adamiak,** Centre for Innovation and Transfer of Natural Sciences and Engineering Knowledge, University of Rzeszow, Pigonia 1 Street, 35-959 Rzeszow, Poland, E-mail: sadamiak@univ.rzeszow.pl
**Wojciech Bochnowski:** E-mail: wobochno@univ.rzeszow.pl, **Andrzej Dziedzic:** E-mail: dziedzic@univ.rzeszow.pl, Centre for Innovation and Transfer of Natural Sciences and Engineering Knowledge, University of Rzeszow, Pigonia 1 Street, 35-959 Rzeszow, Poland
**Ryszard Filip,** Department of Material Science, Rzeszow University of Technology, W. Pola 2 Street, 35-959 Rzeszow, Poland, E-mail: ryfil@prz.edu.pl
**Eugeniusz Szeregij,** Center for Microelectronics & Nanotechnology, University of Rzeszow, Pigonia 1 Street, 35-959 Rzeszow, Poland, E-mail: sheregii@univ.rzeszow.pl

## Introduction

Heat-resistant, nickel-based alloys are the basic materials used in the construction of elements of aircraft engine turbines. The Inconel 625 alloy finds numerous applications in the aircraft industry due to its excellent corrosion resistance and good strength in high temperatures (up to 982 °C [1]) [2, 3]. Elements of jet engine, depending on their location, position and heat rejection, work in temperatures of 700–950 °C. Aluminizing, used since the 1960s, is the oldest method for protecting elements of turbines made of a heat-resistant superalloys against oxidization and corrosion caused by high-temperature working environments [4]. Aluminide coating effectively increases the material's resistance against oxidization in high temperatures by creating a surface layer of $Al_2O_3$ oxides. There are several methods of making the aluminide coating: electroplating, thermal spray, chemical vapor deposition (CVD), pack cementation, hot-dip aluminizing [5]. Diffusion aluminide coatings are commonly used as the protection layers increasing the resistance of blades in modern turbines against corrosion of oxidizing gases in high temperatures. The process of diffusion aluminizing with the contact-gas method (pack cementation) and gas method (out of pack) fulfills the technological criteria required in engine production, but they do not fulfill the ecological standards. Using the CVD method, in which the saturating atmosphere is made in the outer reactor and is delivered in the form of gas aluminum halides to the reactor, enables it to receive the heat-resistant layer of the same chemical composition and phase [6]. The CVD method allows for receiving the aluminide coatings on the nickel-, cobalt- and iron-based alloys with the forecast phase composition and depth [4, 7, 8]. The chemical composition of the gas atmosphere in the reactor has a decisive influence on the microstructure and features of the coating to be created. In the available literature [6, 9–13] there are technologies for creating aluminide sub-layers on the superalloys nickel and titanium bases, there are also defined mechanisms of aluminide coating reinforcement, as well as influences of nickel, aluminum and palladium on the structure, mechanical features and exploitation features of the

tested materials. However, little work has been carried out using the CVD technology for production of an AlNi coating on Inconel 625 alloy. Thus, it is crucial to determine the influence the parameters of CVD process have on the structure and mechanical prosperities of an AlNi coating. In this research the structure of the coatings, the type of fracture, micro- and nanohardness, Young's modulus in the coating layer have been defined. The influence of a load on the microhardness value for the substrate material and aluminide coating made on the superalloy Inconel 625 has been also defined.

## Experimental

Materials used in this research were the cylindrical samples of size ∅17 mm in diameter and 6 mm high, made of the Inconel 625 superalloy. The sampled surfaces were grounded up to SiC no. 800, degreased in isopropyl alcohol and ultrasonically cleaned. The aluminide coating has been created in a low-activity CVD process. The process of making those coatings has been conducted on a BPXPRO3252 device made by IonBond Company on the location at the Aviation Material Research Lab of the University of Technology in Rzeszow. The accepted parameters of the CVD process are presented in Table 1.

**Table 1:** CVD process parameters.

| Lp. | Substrate material | Coatings | Parameters of the coating processing | | |
|---|---|---|---|---|---|
| | | | Temperature, °C | Time, h | Pressure, hPa |
| 1 | Inconel 625 | NiAl | 1,020 | 4 | 150 |
| 2 | | | 1,050 | 8 | 150 |

The first phase of the CVD process was conducted in an external generator at the temperature of 300 °C. Aluminum chloride vapor $AlCl_3$ was produced according to $2Al + 6HCl \rightarrow 2AlCl_3 + 3H_2$ reaction. Subsequently, the saturating atmosphere was transported in a stream of hydrogen gas into the CVD reactor, where superalloy Inconel 625 samples were placed. When the $AlCl_3$ vapor reacted with Ni at the temperature of 1,020 or 1,050 °C grains of intermetallic phase NiAl were formed according to the reaction: $2AlCl_3 + 2Ni + 3H_2 \rightarrow 2AlNi + 6HCl$.

Observations of the microstructure have been made with the use of the scanning electronic microscope Quanta 3D 200i FEI, Helios Nanolab 650 FEI (FEI Laboratory, Eindhoven, NL). The energy dispersive X-ray spectroscopy (EDS) chemical composition analysis has been conducted with the use of the microscope SEM HITACHI S-3400N. Micro- and nanohardness measurements have been performed with the indenter tip – Vickers and Berkovich using a load of the indenter pin of 0.2 N for micro-measurements and 10 mN for nanohardness measurements within the period of 10 s. The imprints have been made with the use of CSM hardness tester. To determine fracture of coatings, samples were subjected to shear. Before shearing, a notch with dimensions of about 0.5 mm × 3 mm × 10 mm was made in the sample. The fracture test has been performed for the samples prepared as shown in Figure 1. The test was conducted with Zwick-Roell Z020 tester and load factor from 0 to 50 kg within 30 s.

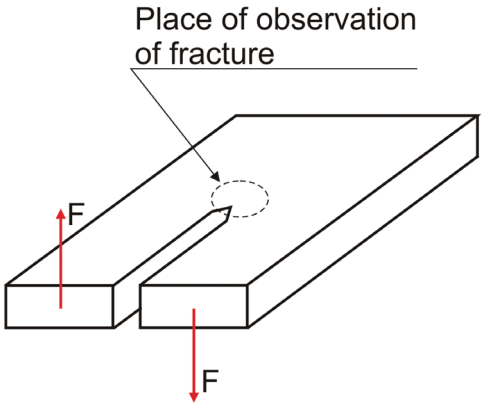


**Figure 1:** The diagram of sample preparation for fracture research.

## Results and discussion

### Structure and chemical composition

The coating structure made on the superalloy Inconel 625 in the CVD process has been analyzed on the scanning electron microscope (SEM). On the observed crosswise microsections (Figure 2) the developed border surface is clearly visible between the base material and the coating.

The metallographic research revealed diversity of the morphology of the resulting coating. The aluminide coating made on the superalloy Inconel 625 in the low-activity CVD process with the parameters of $T = 1{,}020$ °C, $t = 4$ h and $p = 150$ hPa had thickness of 35–37 μm. The aluminide coating made in process with the parameters of $T = 1{,}050$ °C, $t = 8$ h and $p = 150$ hPa had thickness of

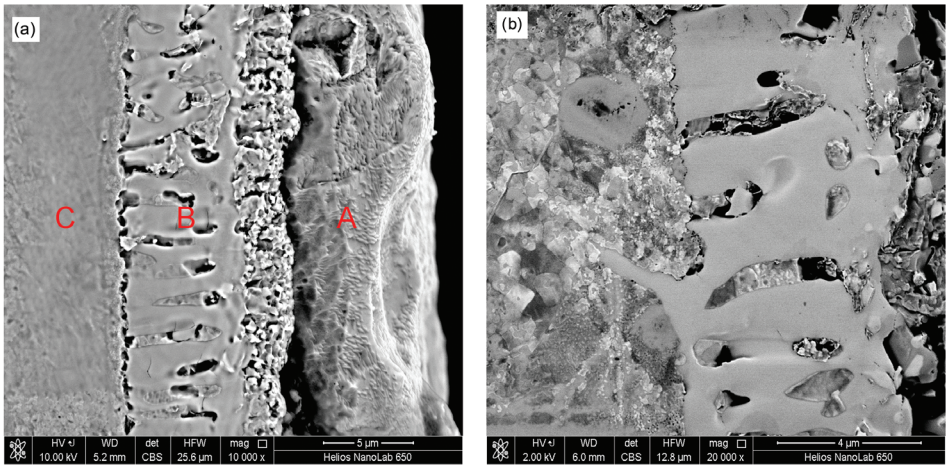


**Figure 2:** The SEM microstructure of a sample section with the aluminide coating produced in the CVD process; A – outer zone, B – interior zone ($T = 1{,}050$ °C, $t = 8$ h, $p = 150$ hPa), C – substrate material.

30–40 µm. The aluminide coating had two-zone structure which was the effect of the cored nickel diffusion from the substrate material to the coating. The outer zone of the aluminide coating (in Figure 2 the "A" zone) had a thickness of about 10–24 µm. In the interior zone of the aluminide coating (in Figure 2 the "B" zone) with thickness of 12–16 µm column structures were observed. Microstructure of the substrate material below the interior zone (Figure 2, area "C") consists of nickel austenite. Figure 3 presents the results of the EDS analysis conducted on a cross section of the coating produced in the 4-h CVD process. Based on the measured atomic content of nickel and aluminum and the AlNi phase diagram (Figure 4(a)) it can be assumed that the outer zone consists mostly of Al-Ni phase [14].

EDS analysis of the chemical composition of the internal zone showed presence of Al, Ni and a high Cr content. Presence of Cr content is the result of diffusion from the substrate material. Taking into account the Al-Ni-Cr phase diagram [15] (Figure 4(b)) and formation energy of phases, the formation of the βAlNi, $\gamma$Ni, $\gamma$'$NiAl_3$, $\delta Al_3Ni$ phase and the Cr containing phases (αCr, $\zeta Al_8Cr_5$, $Al_9Cr_4$, $Al_4Cr$, $Al_7Cr$, $Al_{11}Cr_2$ and $CrNi_2$) is made possible [16].

A characteristic property of the coating produced by the CVD method is surface rumpling (Figure 5). The entire surface shows "wave-like" structure with well-formed bumps. This uneven structure on the AlNi surface is usually explained by its perpendicular rise. On the surface, dents measuring from 3 to 10 µm could be observed. The surface does not show any sharp edges or fractures of the coating. The dents of surface rumpling could be a source of initial corrosion.

The outer zone (for the 4 and 8 h CVD process) showed an increased Al content. Presence of Al was the result of the $AlCl_3 + Ni$ reaction taking place on the surfaces of the samples. The concentration of Al in the outer zone was decreasing in proportion to the distance from the surface of the sample (Figure 6(a) and (b)). Concentration of Ni in the outer zone was constant. The presence of Ni in the zone resulted from the diffusion of the element from the substrate material. The interior zone was characterized by a lower content of nickel toward the outer zone and substrate material. Concentration of Al in this zone was constant and at a low level. In the interior zone an increased concentration of Cr could be observed resulting from diffusion of the element from the substrate material. The EDS analysis conducted in the transverse direction of the AlNi coating showed decreasing concentrations of Cr and Ni and increasing concentration of Al between columnar crystals in the interior zone.

Adhesion of the aluminide coating was determined by fractography. In Figure 7 the microstructure of the fracture of the substrate material and outer and interior zones of the aluminide coating has been presented. The mechanism of cracking is diversified for the particular aluminide coating zones and substrate material. Microstructures of the material fracture for the substrate, outer and interior zones of the aluminide coating obtained for two different variants of CVD process parameters have been presented in Figure 6 ($T = 1{,}050$ °C, $t = 8$ h, $p = 150$ hPa (a–d); $T = 1{,}020$ °C, $t = 4$ h, $p = 150$ hPa (e–h)). The cracking parameter of the outer zone, interior zone and substrate material for the aluminide coating made with the CVD method with the parameters $T = 1{,}050$ °C, $t = 8$ h, $p = 150$ hPa is similar as for the aluminide surface made in

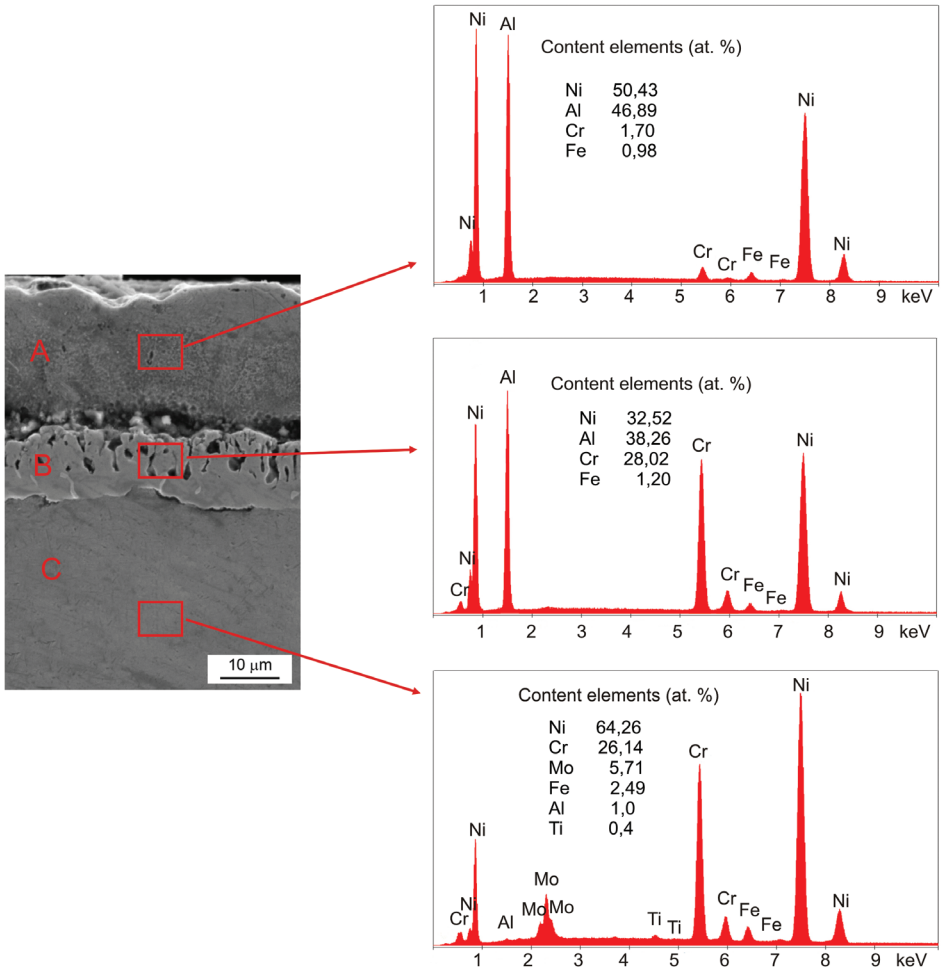


**Figure 3:** EDS spectrum analysis of a coating produced in the 4-h CVD process; A – outer zone, B – interior zone ($T = 1{,}020$ °C, $t = 4$ h, $p = 150$ hPa), C – substrate material.

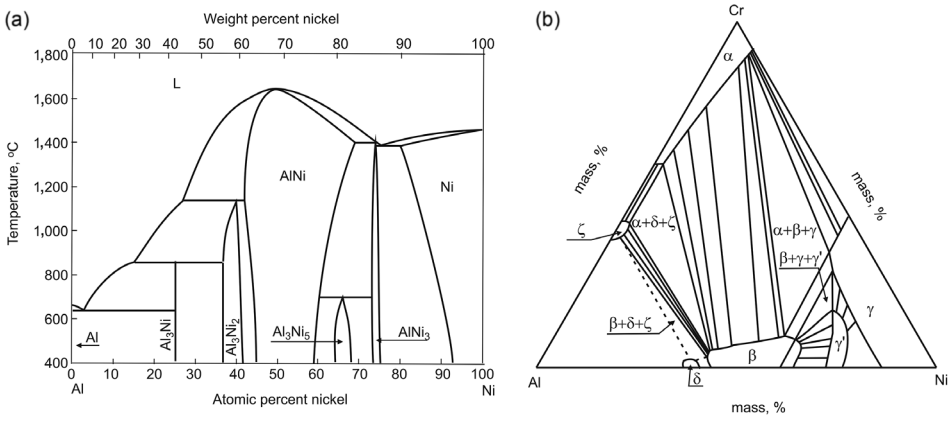


**Figure 4:** (a) Al-Ni phase diagram [14], (b) Al-Ni-Cr phase diagram at 1,025 °C (after [15]).

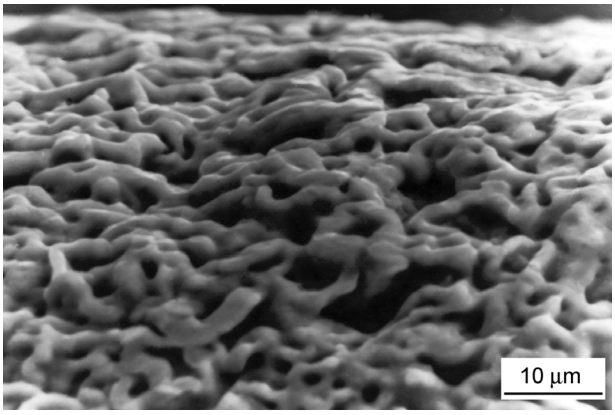


**Figure 5:** A view of the aluminide coating ($T = 1{,}050$ °C, $t = 8$ h, $p = 150$ hPa).

$T = 1{,}020$°C, $t = 4$ h, $p = 150$ hPa. Differences appear only in the fracture thickness of the outer and interior zones due to different times and temperatures of the CVD process (pressure for both CVD process variants was $p = 150$ hPa).

The outer zone of the aluminide coating (for two different variants of CVD process parameters) has been characterized by a fracture of the intercrystalline with localized elements of the transcrystalline cleavage fracture. Another characteristic of the fracture of that zone is large crystal columns of size ranging from few to several micrometers. The interior zone has been built of smaller crystals and also has an intercrystalline fracture. The substrate material has been characterized by a transcrystalline ductile fracture. In samples where the following CVD process parameters were used: $T = 1{,}020$ °C, $t = 4$ h, $p = 150$ hPa, there was a higher number of intercrystalline cracks perpendicular to the surface of the sample (Figure 7(a) and (e)). A large amount of cracks between substrate and coating AlNi (Figure 7(a)) may indicate a smaller adhesion of coating created in 8 h CVD process.

## Nanohardness, microhardness, Young's modulus

During microhardness tests of the thin layers, for example, the aluminide made on the superalloy Inconel 625, the challenge was to address two opposing issues; the applied load of the indenter tip should be the smallest possible in order to avoid the indenter tip penetrating into the layers and differing microhardness by application of a too small load. For choosing the optimal load of the indenter tip there were a series of measurements of the microhardness of the substrate material of superalloy Inconel 625 done by changing the load of the indenter tip from 0.05 to 1 N. The graphic interpretation of the received results has been presented in Figure 8.

On the basis of the research done it has been determined that a significant increase of the material microhardness is present at the loads below 0.2 N. In connection to that, microhardness measurements of the aluminide coating with the indenter tip load of 0.2 N have been done. The results of measurements of the microhardness of the substrate material and individual aluminide coating zones are presented in Figure 9. The largest value of microhardness of about 630 HV0.02 was present in the interior zone of the aluminide coating. Directly under the aluminide coating, in the substrate material, there was an increased hardness (about 330HV0.02) toward the hardness in the deepest areas of the substrate material (about 260HV0.02).

Figure 10 shows the influence of the load factor on the nano- and microhardness values measured using Vickers test method for the aluminide coating zone and substrate material of Inconel 625 superalloy. In the logarithmic scale the change of microhardness is the linear function described (Figure 10). We see that increase of microhardness of substrate and outer zone is similar (directional coefficients of line are respectively: −0.1255 for substrate, −0.1178 for outer zone). In the interior zone there was a greater increase of microhardness, the directional coefficients of line is equal to −0.1498. Similar results of microhardness measurements as a function of load were achieved by Ning et al. [9] who tested AlNi coatings on the Rene N5 substrate material. The average results for the microhardness and the standard deviation from the zones marked, in which the measurements were done, have been presented in Figure 11. The maximum microhardness of the outer zone of the aluminide coating done within 4 h and 8 h on the alloy Inconel 625 was similar, whereas the microhardness of the interior zone was higher, about 90 HV0.02 in a coating with the time of 8 h.

The nanohardness tests were done in accordance with the standard ISO 14577 [17] for the range of the penetration depths $h < 200$ nm. On the basis of the methodology proposed by Oliver and Pharr [18] the following parameters have been determined:

- maximum indentation depth ($h_{max}$),
- permanent indentation depth ($h_p$),
- contact depth of the indenter with the sample at $F_{max}$ ($h_c$),
- contact stiffness ($S$),
- reduced Young's modulus ($E_R$).

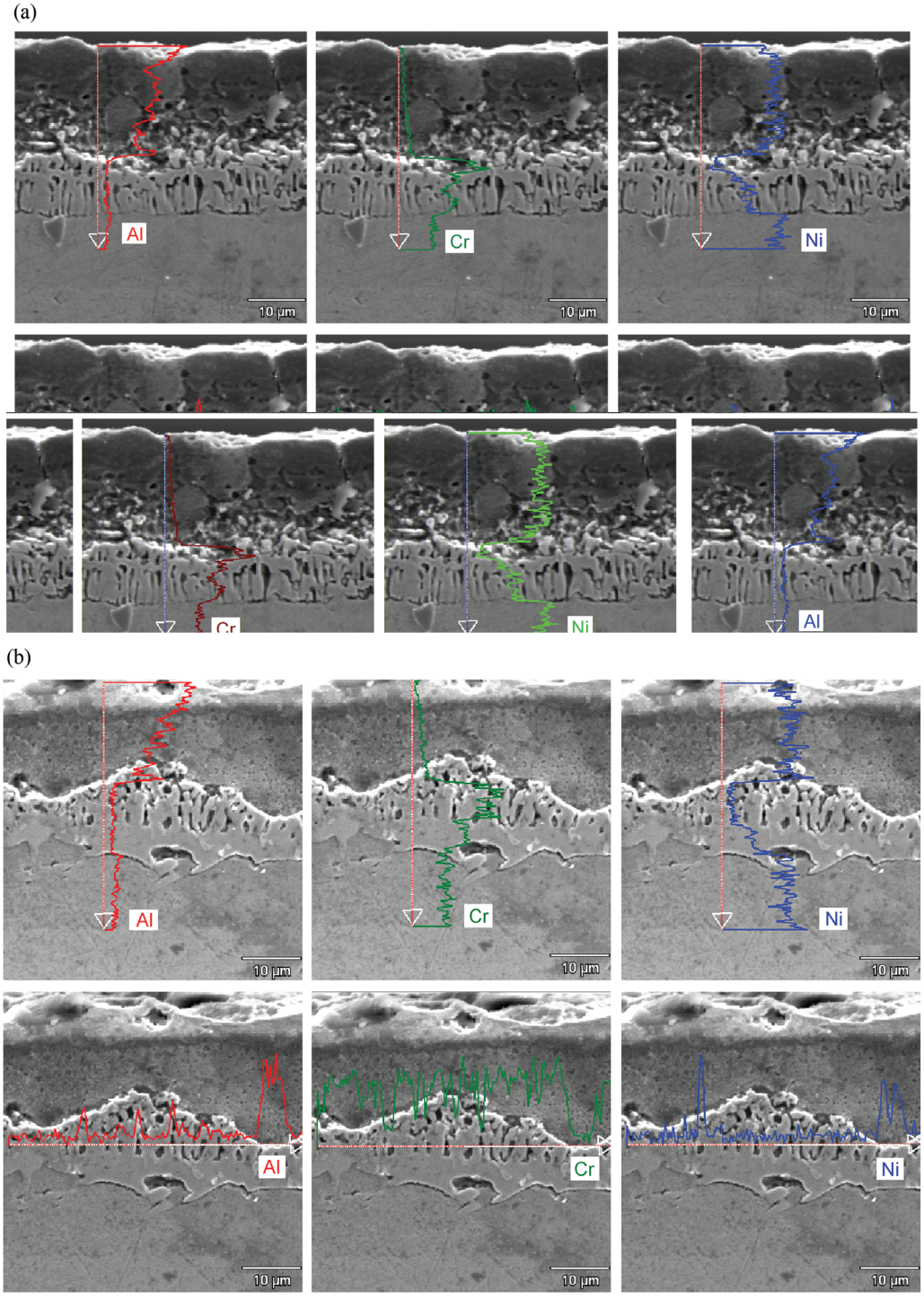


**Figure 6:** The analysis of the chemical composition on the aluminide coating cross section made in the CVD process: (a) $T = 1{,}020$ °C, $t = 4$ h, $p = 150$ hPa, (b) $T = 1{,}050$ °C, $t = 8$ h, $p = 150$ hPa.

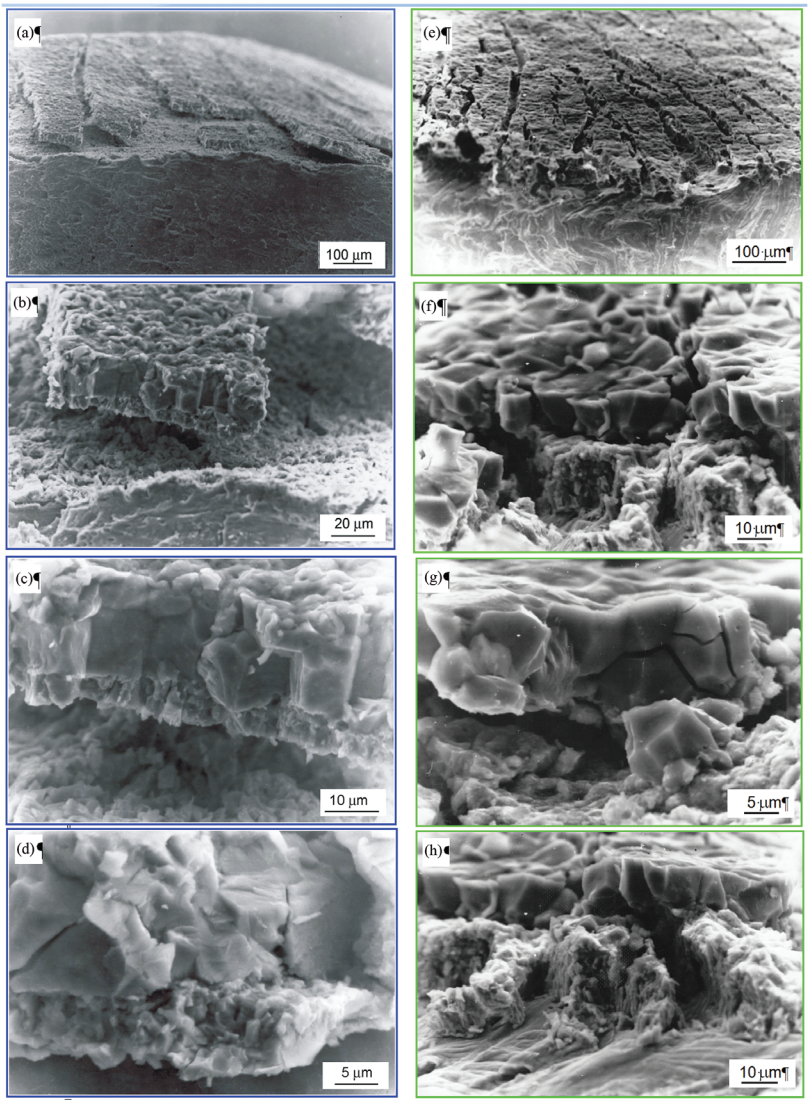


**Figure 7:** Comparison of the microstructure fractures of the outer and interior zones of the aluminide coatings for the two variants of the CVD process parameters; (a)–(d) blue color: $T = 1{,}050$ °C, $t = 8$ h, $p = 150$ hPa; (e)–(h) green color: $T = 1{,}020$ °C, $t = 4$ h, $p = 150$ hPa.

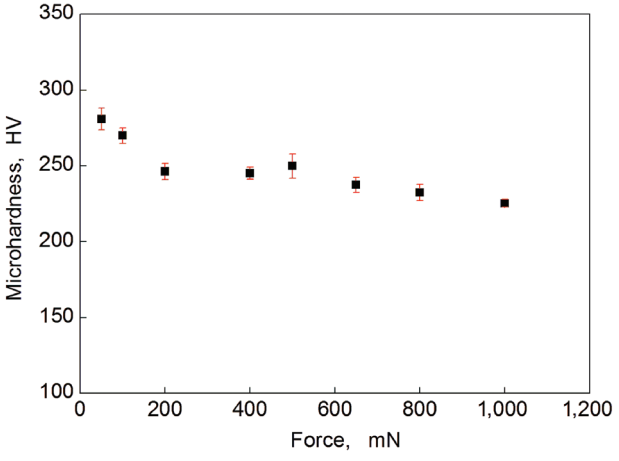


**Figure 8:** The influence of the load of the indenter tip on the microhardness of the superalloy Inconel 625.

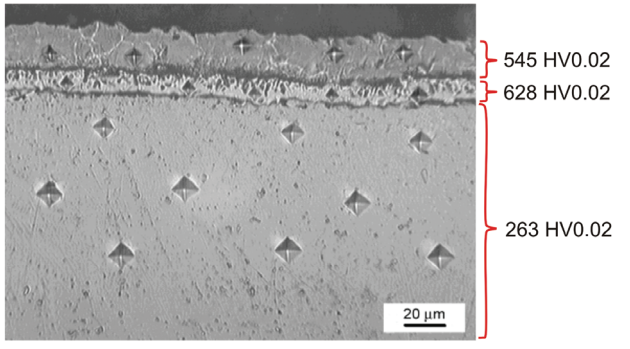


**Figure 9:** Visible Vickers indents in the cross section of the sample material and in particular zones of the aluminide coating ($T = 1{,}050$ °C, $t = 8$ h, $p = 150$ hPa).

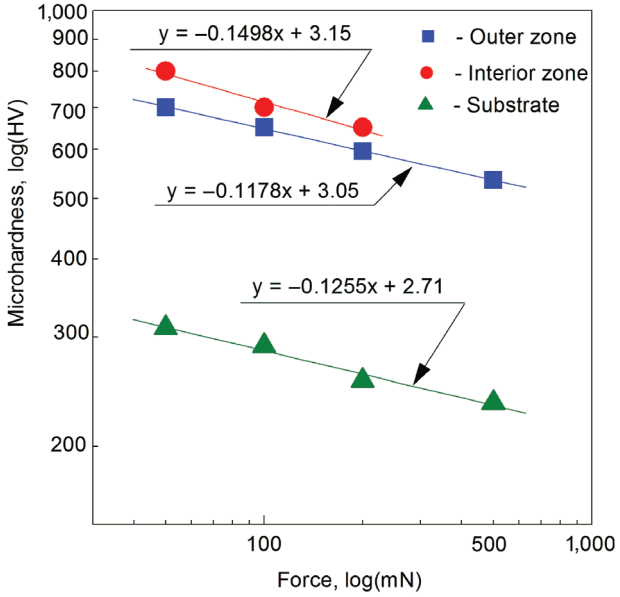


**Figure 10:** Influence of the load on the microhardness value for the substrate material and aluminide coating zones made on Inconel 625 superalloy (parameters of CVD process: $T = 1{,}050$ °C, $t = 8$ h, $p = 150$ hPa).

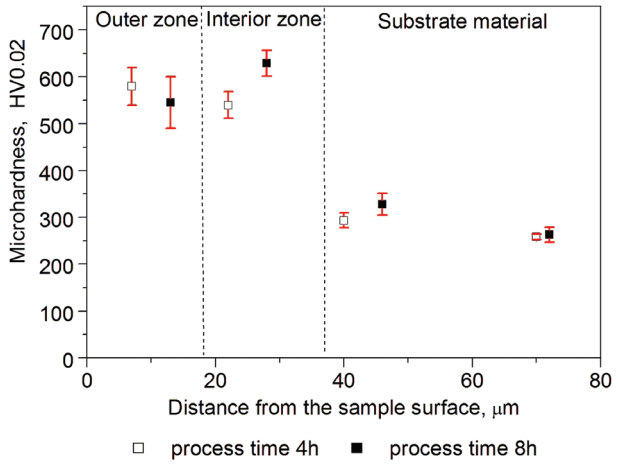


**Figure 11:** Microhardness changes on the aluminide coating on the cross section made with the CVD method for the processing times of 4 h and 8 h.

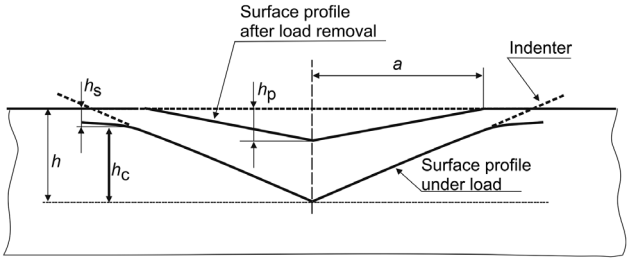


**Figure 12:** The outline of the deformations in the material during the penetrator pressing, $h$ – maximum depth; $h_p$ – permanent indentation depth, $h_c$ – contact depth of the indenter with the sample at $F_{max}$.

The geometrical interpretation of the significant parameters is presented in Figure 12.

The average values of the particular parameters for the substrate material of alloy Inconel 625 and the aluminide coating (8 h CVD process) are presented in Table 2.

Contact depth of the indenter with the sample at $F_{max}$ ($h_c$) calculated from the formula (1) and (2):

$$h_c = h_{max} - \varepsilon \cdot \frac{F_{max}}{S} \tag{1}$$

where $h_{max}$ – maximum indentation depth, $\varepsilon$ – geometric constant, $F_{max}$ – maximum strength, $S$ – contact stiffness.

Contact stiffness designated according to:

$$S = 2E_R\sqrt{\frac{A}{\pi}} \tag{2}$$

where $E_R$ – reduced Young's modulus, $A$ – contact area.

Changes of the load for the particular zones of the tested coating (8 h, 1,050 °C CVD process) and substrate material of superalloy Inconel 625 are presented in Figure 13.

Figure 14 shows measurements of hardness of the aluminide coating produced on the alloy Inconel 625 during 8 h processing, performed with the load of the penetrator 10 mN (nanohardness range) and 200 mN (microhardness range). There is an ostensible increase of the hardness visible in the aluminide coating and the substrate material.

**Table 2:** Average values of the parameters defined in the nanohardness measurements of the coating zones and substrate material (8 h CVD process).

| Zones | $F_{max}$ [mN] | $h_{max}$ [nm] | $h_c$ [nm] | $h_r$ [nm] | $h_p$ [nm] | $\varepsilon$ – | $A_p$ nm$^2$ | $S$ – |
|---|---|---|---|---|---|---|---|---|
| Outer zone | 10 | 221 | 196 | 187 | 169 | 0.74 | $1.23 \times 10^6$ | 0.345 |
| Interior zone | 10 | 190 | 155 | 144 | 123 | 0.76 | $7.78 \times 10^6$ | 0.220 |
| Substrate material of Inconel 625 | 10 | 288 | 262 | 253 | 241 | 0.76 | $1.90 \times 10^6$ | 0.292 |

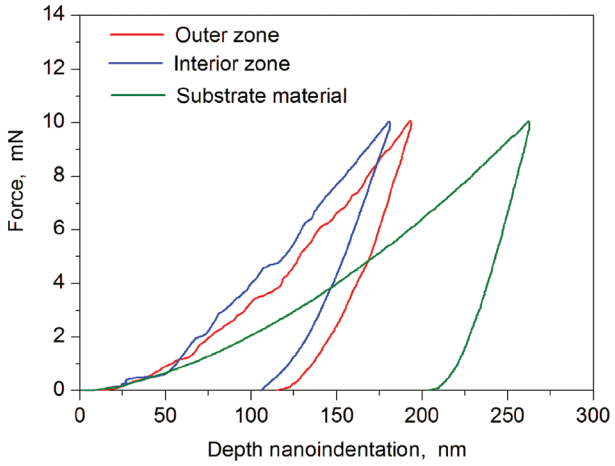


**Figure 13:** The load changes in the depth function of the penetrator in different zones of the aluminide coating and substrate material (core) of superalloy Inconel 625, process time 8 h.

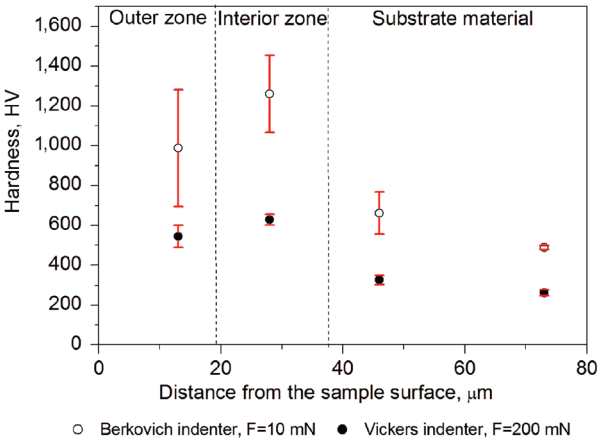


**Figure 14:** The microhardness and nanohardness range, measurement on the cross section of the aluminide coating created with the CVD method, process time 8 h.

The reduced Young's modulus ($E_R$) has been designated for the substrate material and aluminide coating created with the CVD method with duration of 8 h. The obtained average values of the reduced Young's modulus of the tested sample are presented in Figure 15. The maximum module value $E_R$ was received in the outer zone of the aluminide coating and was on $E_R = 314$ GPa. In the interior zone the smaller values were received up to about 257 GPa, and in the substrate material $E_R = 180$ GPa.

## Conclusion

1. The aluminide coating has developed surface on the border with the substrate material. The created aluminide coating has a two-zone construction: outer zone and interior zone. Interior consists of column crystals.
2. In defining microhardness of the aluminide coating one should include the optimal selection of the indenter's load. The nano- and microhardness analysis shows influence of the penetrator load on the hardness values within small loads.
3. The fracture mechanism was different for the respective zones of the aluminide coating and the substrate material. The outer zone of the aluminide coating is characterized by an intercrystalline fracture, with a small contribution of transcrystalline fracture within individual grains (large crystallites in the bottom of the zone). The interior zone was composed of smaller crystallites, has also an intercrystalline fracture. The substrate material exhibited a ductile transcrystalline fracture.

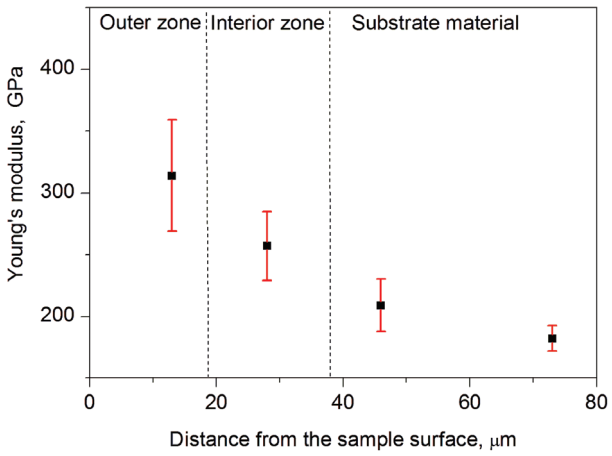


**Figure 15:** Reduced Young's modulus measurement on the cross section of the aluminide coating and substrate material created with the CVD method, process time 8 h.

**Funding:** Financial support of Structural Funds in the Operational Program – Innovative Economy (IE OP) financed from the European Regional Development Fund – Project "Modern material technologies in aerospace industry", No. POIG.0101.02-00-015/08 is gratefully acknowledged.

## References

1. Product Handbook of High-Performance, Special Metals Corporation (2008).
2. Xu F, Lv Y, Liu Y, Xu B, He P. Effect of heat treatment on microstructure and mechanical properties of inconel 625 alloy fabricated by pulsed plasma arc deposition. Phys Procedia 2013;50:48–54.

3. Rai SK, Kumar A, Shankar V, Jayakumar T, Rao KS, Raj B. Characterization of microstructures in Inconel 625 using X-ray diffraction peak broadening and lattice parameter measurements. Scr Mater 2004;51:59–63.
4. Yavorska M, Poręba M, Sieniawski J. Development of microstructure of aluminide layer on base superalloys in the low-activity CVD process. Mater Eng (Pol) 2008;6:749–52.
5. Cheng WJ, Wang CJ. Observation of high-temperature phase transformation in the, Si-modified aluminide coating on mild steel using EBSD. Mater Charact 2010;61:467–73.
6. Poręba M, Ziaja W, Kubiak K. Microstructure and heat resistance of aluminide coating developed on rené 77 superalloy in low-activity CVD process. Mater Eng (Pol) 2008;6:753–6.
7. Pomeroy MJ. Coatings for gas turbine materials and long term stability issues. Mater Des 2005;26:223–31.
8. Tolpygo VK, Clarke DR. On the rumpling mechanism in nickel-aluminide coatings. Part II: characterization of surface undulations and bond coat swelling. Acta Mater 2004;52:5129–41.
9. Ning B, Stevenson ME, Weaver ML, Bradt RC. Apparent indentation size effect in a CVD aluminide coated Ni-base superalloy. Surf Coat Technol 2003;163–164:112–17.
10. Wang CJ, Chen SM. Microstructure and cyclic oxidation behavior of hot dip aluminized coating on Ni-base superalloy Inconel 718. Surf Coat Technol 2006;201:3862–6.
11. Lia MJ, Suna XF, Guana HR, Jianga XX, Hua ZQ. The degradation of (Ni,Pd)Al coatings on superalloy IN738 during isothermal oxidation. Surf Coat Technol 2004;185:172–7.
12. Tolpygo VK, Clarke DR. Rumpling of CVD (Ni,Pt)Al diffusion coatings under intermediate temperature cycling. Surf Coat Technol 2009;203:3278–85.
13. Tacikowski M, Sitek R, Sikorski K, Wierzchoń T. Structure of Al-Ni intermetallic composite layers produced on the Inconel 600 by the glow discharge enhanced-PACVD metod. Intermetallics 2009;17:1098–104.
14. Huang W, Chang YA. A thermodynamics analysis of the Ni-Al systems. Intermetallics 1998;6:487–98.
15. ASM Handbook. Alloy phase diagrams. Novelty, OH: ASM International, 1992.
16. Comptona DN, Cornisha LA, Witcombb MJ. The effect of microstructure on hardness measurements in the aluminium-rich corner of the Al–Ni–Cr system. J Alloys Compd 2001;317–318:372–8.
17. Standard ISO/FDIS 14577-1:2002. Metallic materials – instrumented indentation test for hardness and materials parameters, 2002.
18. Oliver WC, Pharr GM. An improved technique for determining hardness and elastic modulus using load and displacement sensing indentation experiments. J Mater Res 1992;7:1564–83. Copyright © Materials Research Society 1992.